

Observation of nanojet-induced modes with small propagation losses in chains of coupled spherical cavities

A. M. Kapitonov

*Center for Optoelectronics and Optical Communications, University of North Carolina at Charlotte,
9201 University City Boulevard, Charlotte, North Carolina 28223, USA*

V. N. Astratov

*Department of Physics and Optical Science, Center for Optoelectronics and Optical Communications, University of
North Carolina at Charlotte, 9201 University City Boulevard, Charlotte, North Carolina 28223, USA*

Received August 22, 2006; revised October 30, 2006; accepted October 31, 2006;
posted November 7, 2006 (Doc. ID 74324); published January 26, 2007

Nanojet-induced modes (NIMs) and their attenuation properties are studied in linear chains consisting of tens of touching polystyrene microspheres with sizes in the 2–10 μm range. To couple light to NIMs we used locally excited sources of light formed by several dye-doped fluorescent microspheres from the same chain of cavities. We directly observed the formation and propagation of NIMs by means of the scattering imaging technique. By measuring attenuation at long distances from the source, we demonstrate propagation losses for NIMs as small as 0.5 dB per sphere. © 2007 Optical Society of America
OCIS codes: 230.3990, 230.7370, 250.5300, 350.3950.

Waveguides can be created in photonic microstructures using different optical phenomena such as total internal reflection in layered structures, photonic bandgaps in photonic crystal waveguides, and tight binding between high-quality (Q) cavities in coupled resonator optical waveguide¹ structures. Recently it has been argued² that spherical or cylindrical cavities arranged as a linear chain provide optical transport due to two different mechanisms: (i) tight binding^{3,4} between whispering gallery modes (WGMs), (ii) coupling occurring as a result of focusing produced by cavities operating as a series of periodically coupled microlenses. In the latter case each microsphere produces a focused spot termed the “nanoscale photonic jet,”^{5,6} with elongated shape and subwavelength lateral size. In a chain of spheres such nanojets result in periodic modes, called nanojet-induced modes (NIMs) in this Letter.

Experimentally, strong coupling⁷ between WGMs and their band structure effects^{8,9} have been observed in systems of supermonodispersive cavities selected using spectroscopic characterization. In size-mismatched bispheres and in the chains of disordered cavities, WGM-related optical coupling was observed^{10,11} by use of evanescently coupled dye-doped spherical cavities pumped above the lasing threshold for WGM peaks.

The properties of NIMs are very different from WGMs since they are not resonant modes and because of the radiative nature of photonic nanojets. The NIMs, however, are not well studied at present. Some properties of tightly focused beams were studied in the case of single immersion lens,¹² and some nonresonant optical transport phenomena were observed in coupled submicrometer spheres¹³; however, the existence of NIMs has not been clearly demonstrated previously.

In the present work we directly observed NIMs and studied their properties in very long chains consisting of several tens of polystyrene spheres with sizes in the 2–10 μm range. To couple light to these modes we used emission of several dye-doped fluorescent microspheres excited below the lasing threshold for WGMs locally inside the chains. By directly observing a series of photonic jets at the shadow side of multiple spheres, a characteristic feature of NIMs, we demonstrate that the fluorescence from the source is gradually converted into NIMs away from such a source. We demonstrate less than 0.5 dB per sphere propagation losses for NIMs.

Linear arrays of monodispersive ($\sim 3\%$ size dispersion) polystyrene spheres (Green Fluorescent, Duke Scientific Corp.) with refractive index $n=1.59$ and mean diameters 1.9, 2.2, 2.9, 5.0, and 10.1 μm were deposited on glass substrates by using a technique of self-assembly directed by microflows of water suspension of spheres, as illustrated in Fig. 1. In this method the “pinning” points forming pipelike flows¹⁴ are nucleated by the spheres of larger size. In the course of water evaporation¹⁵ these flows gradually shrink, reaching the size of an individual sphere in cross section, causing the formation of long chains of touching spheres.

The synthesis was monitored and the samples were optically characterized with a fluorescent (FL) inverted IX-71 Olympus microscope. The beads were internally doped with green FL dye (emission max at

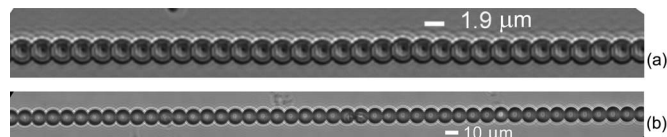


Fig. 1. Optical images of sections of chains of polystyrene spheres with mean diameter (a) 1.9 and (b) 10.1 μm .

508 nm). The FL excitation was provided in the range 460–500 nm. An excitation spot with adjustable size was formed by the spatial filter, and it was focused on the chain of spheres with a 60× objective (NA=0.9). The distribution of the intensity was relatively uniform within the excitation spot and with very steep terminations at the edges of the spot, thus allowing the creation of a built-in source of light formed by several pumped spheres inside the chain.

The intensity of excitation was well below the threshold for lasing WGMs. Under these conditions only a small fraction (not more than a few percent, since the beads are dye doped throughout the volume) of the total FL intensity is coupled to WGMs, and most of the intensity is emitted into radiative modes with a broad (500–570 nm) spectrum. A part of this intensity is coupled to modes propagating in the chain away from the source. These modes can be visualized with a microscope due to the scattering in the vertical direction. The images were registered by CCD video camera with variable exposure time and 12 bit dynamic range.

The formation of NIMs is demonstrated in Fig. 2. The source was formed by exciting several spheres inside the 2.9 μm chain, as illustrated in Fig. 2(a). Light propagation in the unexcited part of the chain results in efficient focusing and scattering in tiny volumes close to the touching points of the neighboring spheres, visible as bright spots in Fig. 2(b). It should be noted that the propagation is associated with gradual narrowing of such bright spots with increas-

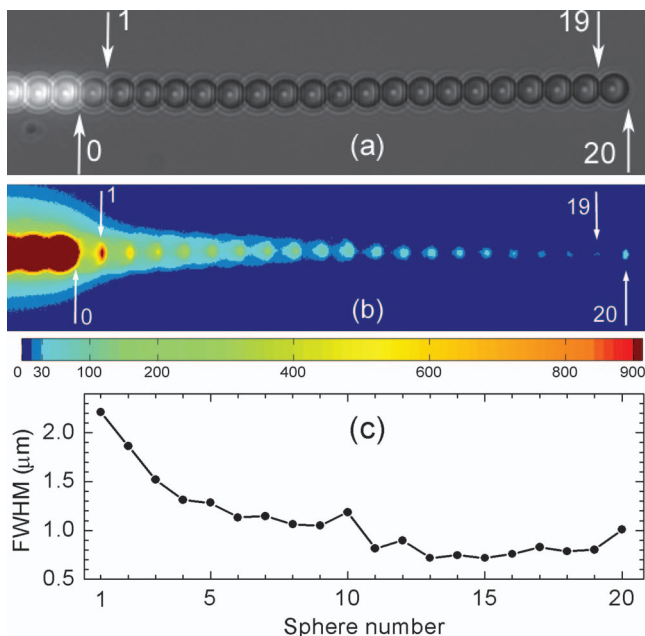


Fig. 2. Visualization of NIMs in a locally excited chain of 2.9 μm spheres. (a) Image obtained with the background white-light illumination. Three spheres (left) are pumped. (b) Same chain imaged without background illumination due to propagation and scattering of light originating from the FL source. To display weak intensities we used a color bar (0–900 counts). The maximum intensity from excited spheres (to the left from the 0 mark) is about 3500. (c) Cross-sectional FWHM of bright spots measured in unexcited spheres perpendicular to the chain.

ing distance from the source as illustrated in Fig. 2(c). The narrowing of bright spots is most pronounced in the first decade of spheres adjacent to the source, where one can expect a mode conversion into NIMs with corresponding mode conversion losses to occur. As shown in Fig. 2(c), beyond the first decade of spheres the transverse size of these bright spots appears saturated at the level of ~0.7 μm, which represents the resolution limit of our setup. The actual size of photonic jets formed by $n=1.6$ spheres with sizes of several wavelengths should be even smaller according to theory.^{5,6} An increase of the jet intensity in the end cavity takes place due to stronger scattering caused by the increased index contrast at the last interface of the chain.

To study propagation losses in such chains we found the maxima of the intensity of nanojet images and plotted them for sequential spheres along the chains, as illustrated in Fig. 3. All data are normalized on the intensity of the maximum observed in the first sphere that is not excited (position 1 in Fig. 2). Different attenuation curves in Fig. 3 represent cases with different numbers of spheres excited in the FL source region. The attenuation curves in Fig. 3 display a series of dependencies that are more complicated than a single exponent. In the first several spheres the mode conversion losses are the dominant factor of attenuation, as is evident from the maximal slope of the attenuation curves in this region. Attenuation per sphere decreases with increasing distance from the excited area due to the spatial filtering of modes passing through the array of microlenses. Since the formation of nanojets is nearly completed after the first decade of spheres, as can be seen from Fig. 2(c), the losses measured in more distant spheres become indicative of the propagation losses for NIMs. By comparing the curves in Fig. 3, it is seen that the larger the number of spheres that was used in the source region, the less attenuation we can detect at long distances from such extended sources. This behavior originates from the superposition of contributions of individual spheres comprising such extended source, as illustrated in Fig. 3(a).

To extract light attenuation parameters from the experimental data in Fig. 3 we employed a semi-empirical double-exponent fitting function:

$$I = I_1 10^{-0.1\beta_1 N} + I_2 10^{-0.1\beta_2 N}, \quad (1)$$

where I_1 and I_2 are intensities of two exponential components, β_1 and β_2 are their attenuation levels per individual sphere (in dB), and N is the propagation distance expressed in number of spheres. Although this model is only an approximation to the shape of the decay curves in Fig. 3, it has a transparent physical meaning. The first exponent can be associated with mode conversion losses occurring in the first several spheres, whereas the second exponent provides an estimate of the propagation losses for NIMs at much longer distances from the source.

In Fig. 4 we show attenuation levels β_1 and β_2 for two exponential components and their relative decay amplitudes I_1/β_1 and I_2/β_2 , representing the amount of light scattered by a given channel. The data for

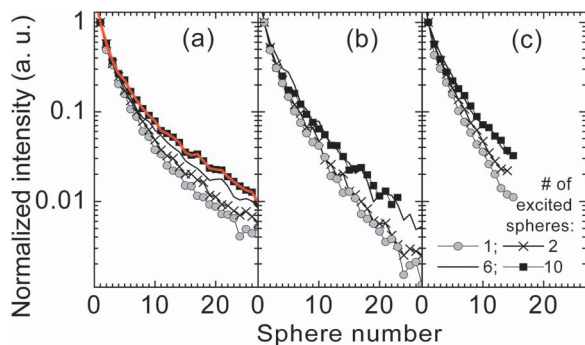


Fig. 3. Intensity maxima of scattered light measured in a sequence of nonexcited spheres along the chain. The data are normalized on the intensity of the first maximum (position 1 in Fig. 2). The size of the spheres in chains: (a) 1.9, (b) 2.9, (c) 10.1 μm . Different curves represent cases with different number of excited spheres in the FL source region. The red curve in (a) is the simulation of 10 spheres as a superposition of 10 consecutively shifted attenuation curves measured from a single sphere source.

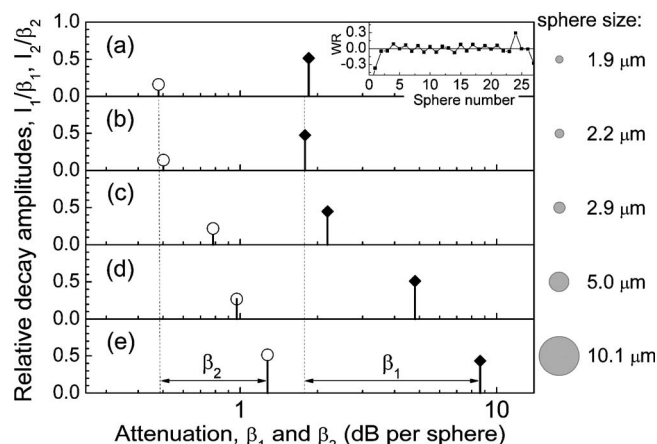


Fig. 4. Fit parameters of double-exponential model [Eq. (1)] found in the case of a single sphere excited in chains of spheres of the following sizes: (a) 1.9, (b) 2.2, (c) 2.9, (d) 5.0, and (e) 10.1 μm . The horizontal axis represents attenuation per sphere β_1 (solid rhombs) and β_2 (empty circles) for two exponential components. The vertical axis displays relative decay amplitudes I_1/β_1 and I_2/β_2 of these components. The inset in (a) shows weighted residuals (WR) of the fit.

chains with sphere sizes in 1.9–10.1 μm range are summarized in Fig. 4 for the case of a built-in source of light formed by a single excited sphere. For all studied chains the strong initial light loss in the vicinity of the FL source is characterized by attenuation parameters β_1 which are of the order of several dB per sphere. Further propagation of NIMs is found to occur with significantly lower attenuation β_2 (≤ 1 dB per sphere). It is interesting to note that our experimental data exhibit a decrease of light attenuation for both exponential components for smaller spheres. For the chain formed by 1.9 μm spheres the NIMs propagation losses drop to a level of 0.48 dB

per sphere. The level of NIMs losses in our samples is determined by structural imperfections such as slight deviations from the coaxial alignment of cavities. Further experimental and theoretical work is required to reveal the intrinsic radiation loss of NIMs.

The reduced attenuation observed for smaller spheres can be explained by the increasing focusing strength of spherical microlenses with sizes of the order of a few wavelengths (λ) compared with larger spheres. In the limit of geometrical optics (sphere diameter exceeds several tens of λ) the index of refraction of sphere must be equal to 2 to provide the maximum intensity of focused light at the “shadow” surface of a sphere. It has been demonstrated^{5,6} that with a decrease of the diameter to a few λ the required value of the refractive index drops to 1.6, which is very close to the refractive index of polystyrene.

The authors thank M. A. Fiddy, M. S. Skolnick, T. Itoh, and S. P. Ashili for stimulating discussions. This work was supported by Army Research Office grant W911NF-05-1-0529 and by National Science Foundation grant CCF-0513179 as well as in part by funds provided by the University of North Carolina at Charlotte. A. M. Kapitonov (amkapito@uncc.edu) was partly supported by DARPA grant W911NF-05-2-0053. The authors are thankful to Duke Scientific Corporation for donating microspheres for this research.

References

1. A. Yariv, Y. Xu, R. K. Lee, and A. Scherer, *Opt. Lett.* **24**, 711 (1999).
2. Z. Chen, A. Taflove, and V. Backman, *Opt. Lett.* **31**, 389 (2006).
3. S. Deng, W. Cai, and V. N. Astratov, *Opt. Express* **12**, 6468 (2004).
4. A. V. Kanaev, V. N. Astratov, and W. Cai, *Appl. Phys. Lett.* **88**, 111111 (2006).
5. Z. Chen, A. Taflove, and V. Backman, *Opt. Express* **12**, 1214 (2004).
6. S. Lecler, Y. Takakura, and P. Meyrueis, *Opt. Lett.* **30**, 2641 (2005).
7. T. Mukaiyama, K. Takeda, H. Miyazaki, Y. Jimba, and M. Kuwata-Gonokami, *Phys. Rev. Lett.* **82**, 4623 (1999).
8. Y. Hara, T. Mukaiyama, K. Takeda, and M. Kuwata-Gonokami, *Phys. Rev. Lett.* **94**, 203905 (2005).
9. M. Möller, U. Woggon, and M. V. Artemyev, *Opt. Lett.* **30**, 2116 (2005).
10. V. N. Astratov, J. P. Franchak, and S. P. Ashili, *Appl. Phys. Lett.* **85**, 5508 (2004).
11. S. P. Ashili, V. N. Astratov, and E. C. H. Sykes, *Opt. Express* **14**, 9460 (2006).
12. D. Terris, H. J. Mamin, D. Rugar, W. R. Studenmund, and G. S. Kino, *Appl. Phys. Lett.* **65**, 388 (1994).
13. T. Fujimura, K. Edamatsu, T. Itoh, R. Shimada, A. Imada, T. Koda, N. Chiba, H. Muramatsu, and T. Ataka, *Opt. Lett.* **22**, 489 (1997).
14. K. Y. Suh, *Small* **2**, 832 (2006).
15. V. N. Manoharan, M. T. Elsesser, and D. J. Pine, *Science* **301**, 483 (2003).